Influence of Charged Surfaces on the Morphology of DNA Condensed with Multivalent Ions

K. Besteman, K. van Eijk, I. D. Vilfan, U. Ziese, S. G. Lemay
Kavli Institute of Nanoscience, Delft University of Technology, 2628 CJ Delft, The Netherlands

Received 5 April 2007; revised 27 June 2007; accepted 3 July 2007
Published online 11 July 2007 in Wiley InterScience (www.interscience.wiley.com). DOI 10.1002/bip.20806

ABSTRACT:

DNA in solution can be condensed into dense aggregates by multivalent counterions. Here we investigate the effect of a nearby surface on the morphology of DNA condensates. We show that, contrary to what has often been assumed, interactions between DNA condensates and the surface can strongly influence the observed morphology. This limits the usefulness of surface probes such as atomic force microscopy for studying the morphology of condensates in bulk solution. Surprisingly, we find that the most negatively charged surface disturbs the condensate morphology most, suggesting that the microscopic mechanism resulting in DNA condensation is also responsible for the attractive force between DNA and the surface. © *2007 Wiley Periodicals, Inc. Biopolymers 87: 141–148, 2007.*

Keywords: DNA; condensation; atomic force microscopy; multivalent ions

This article was originally published online as an accepted preprint. The "Published Online" date corresponds to the preprint version. You can request a copy of the preprint by emailing the Biopolymers editorial office at biopolymers@wiley.com

Correspondence to: S. G. Lemay; e-mail: s.g.lemay@tudelft.nl
Contract grant sponsors: Stichting voor Fundamenteel Onderzoek der Materie (FOM), Netherlands Organization for Scientific Research (NWO)

INTRODUCTION

DNA in solution can condense into compact structures in the presence of a sufficiently high concentration of multivalent cations.[1] This multivalent-ion-induced DNA condensation was first observed with the naturally occurring polyamine spermidine[2] which, together with other polyamines, is involved in several cellular processes including DNA compaction in vivo.[3] DNA compaction by polycations has also been identified as a promising system for gene delivery.[4]

It is mostly believed that the short range interaction leading to DNA condensation results from an inhomogeneous distribution of counterions causing oscillations of the polarity of the charge along the length of the DNA.[5–10] Proposals for the origin of this charge modulation include dynamic fluctuations of the counterion distribution,[6,8] the intrinsic helicity of DNA,[7] and the formation of a strongly correlated liquid (SCL) of multivalent counterions.[9,10] Directly probing the microscopic interaction between DNA molecules experimentally has however proven difficult because of the short length scales involved.

One of the main approaches being pursued to infer the microscopic mechanism behind DNA condensation consists in investigating the morphology of DNA condensates and its evolution over time. Several imaging techniques have been applied to this problem. Using electron microscopy, toroidal, rod-like and sphere-like structures were reported for DNA condensed with the trivalent ions spermidine and cobalt hexamine and the quadrivalent ion spermine.[2,11,12] In these measurements, the DNA was condensed in solution and deposited on a hydrophobic carbon grid, then stained to obtain contrast, and finally fixed on the surface with ethanol. Most of the observed structures were three-dimensional and appeared largely undistorted by the presence of the imaging surface. Considerable further support for the hypothesis that the observed structures resemble those in bulk solution was given by the cryoelectron microscopy work of Hud and Downing.[13]

Another powerful imaging technique frequently used for the study of the morphology of condensed DNA is atomic force microscopy (AFM).[14] A variety of morphologies, including toroid-like, rod-like and so-called flower-like structures have been observed using AFM for DNA condensed with spermine and spermidine,[15–17] cobalt hexamine,[18] and several other multivalent cations.[19,20] Although some of the observed morphologies resemble those observed with electron microscopy, most observations with AFM show more poorly defined structures that are often relatively flat. It has been argued that the flower-like structures are early intermediates in the condensation pathway.[15] Similar structures were also observed for DNA condensed using several polycations considered promising for gene delivery.[21–25] Finally, DNA has been observed to condense in the presence of mobile cationic surface groups.[26–28]

Advantages of AFM are that no staining is required to observe the condensates and that imaging can be performed in liquid without drying the sample (although most existing AFM studies of DNA condensation have nonetheless been done in air for practical reasons). This technique however requires the condensates to be attached to a surface; most studies use mica as the imaging surface as it is very flat, hydrophilic, and readily binds DNA condensates. However, It remains unclear to what extent the observed structures reflect those present in bulk or are influenced by the nearby surface. Nontrivial interactions can be expected since the same physical mechanism that causes DNA–DNA attraction and condensation can also potentially mediate an attractive interaction between DNA and the negatively charged mica.

Here we investigate the effect of a nearby surface on the morphology of DNA condensates. We obtained high-quality images of DNA condensates prepared over a broad range of concentrations of different multivalent ions and deposited on surfaces with different properties. We conclude that the morphology of the condensates is strongly influenced by the nearby surface, significantly limiting the applicability of AFM as a probe of the morphology of multivalent-ion-induced DNA condensates in solution. Counter-intuitively, the most negatively charged surface, bare mica, exhibits the strongest attraction for negatively charged DNA. This suggests that the same counterion-mediated interaction responsible for DNA condensation also dominates DNA-surface interactions.

MATERIALS AND METHODS

We have used four different positively charged multivalent cations to condense DNA. These included the two trivalent ions cobalt sepulchrate ($[CoC_{12}H_{30}N_8]^{3+}$, cosep) and cobalt hexamine ($[Co(NH_3)_6]^{3+}$, cohex), as well as the biologically relevant trivalent and quadrivalent polyamines spermidine ($[C_7N_3H_{22}]^{3+}$) and spermine ($[C_{10}N_4H_{30}]^{4+}$). All ions were ordered from Sigma as chloride salts and used as received.

We present AFM data for three different imaging surfaces, freshly cleaved muscovite mica (bare mica), freshly cleaved graphite, and mica coated with poly-L-lysine (PL). Bare mica is negatively charged in water and DNA does not adsorb to it in the absence of multivalent ions. Graphite is very hydrophobic with a slight negative charge at neutral pH. Finally, adsorbing PL on mica yields a positively charged surface and thus allows DNA to bind even in the absence of multivalent ions. This surface is commonly employed to image DNA with AFM. We prepared PL-coated mica surfaces by incubating a 5 μL droplet of 0.1% PL (molecular weight 70,000–150,000) in deionized, milli-Q-filtered water (milli-Q water) on freshly cleaved muscovite mica for 30 s, after which the droplet was flushed off with milli-Q water and the surface was blown dry in a stream of nitrogen. Using AFM force spectroscopy,[29,30] we experimentally verified that the PL-coated mica was positively charged.

DNA samples were prepared in an identical manner for all measurements. Double-stranded 1.5 kbp DNA fragments were produced by PCR using λ-DNA as a template and primer sequences 5′-GTAAAGCGCCACGCTCC and 5′-TGATATTGCCAAAACAGAGCTG, and purified using gel extraction. Solutions containing 1 ng/μL DNA, 10 m*M* TRIS (Tris Hydroxymethylaminoethane) buffer with pH 7.5, and a concentration of multivalent ions in the range between 10^{-6} and 1*M* were prepared. After a 5 min incubation time, 5 μL of solution was deposited on the surface. Imaging was done both in air and in liquid environment. For imaging in air the droplet was flushed off after 1 min with milli-Q water and dried in a stream of nitrogen. For imaging in liquid the droplet was flushed off after 1 min with a solution containing 10 m*M* TRIS and the same concentration of multivalent ions as the condensing solution. Subsequently the dry or wet substrates were imaged with a Digital Instrument NanoScope IV AFM using tapping mode. For dry imaging Olympus Micro cantilevers (OMCL-C160TS) with a spring constant of 42 N/m (as indicated by the manufacturer) were used. Wet imaging was done using Veeco Microlever probes (MLCT-AUHW) with a spring constant of 0.03 N/m (as indicated by the manufacturer).

Multivalent cations from the DNA solution also participate in screening the negative surface charge of bare mica and graphite. For low bulk concentrations of multivalent ions, this accumulation of multivalent ions at the surface lowers the bulk concentration and could thereby hinder condensation. We verified that this was not a significant factor in this experiment at 100 μM spermidine by pretreating bare mica with 100 μM spermidine in 10 m*M* TRIS solution to saturate the mica with multivalent ions before depositing a droplet containing the DNA and 100 μM spermidine. No change in behavior was observed, indicating that depletion of the bulk solution does not play a major role in our experiments.

Dynamic light scattering (DLS) measurements were performed using a Zetasizer Nano ZS apparatus (Malvern Instruments) to independently determine the hydrodynamic diameter of the DNA condensates in the solution. Volumes of 1 mL of the same solutions as used for AFM were prepared. After a variable incubation time the DLS measurement was performed in a disposable cuvette.

Transmission electron microscopy (TEM) was performed using a Philips CM300 UT FEG instrument at 300 kV. TEM samples were prepared by depositing 5 μL of solution, as used for AFM on a carbon-coated grid, incubating for 10 min and staining for 1 min with

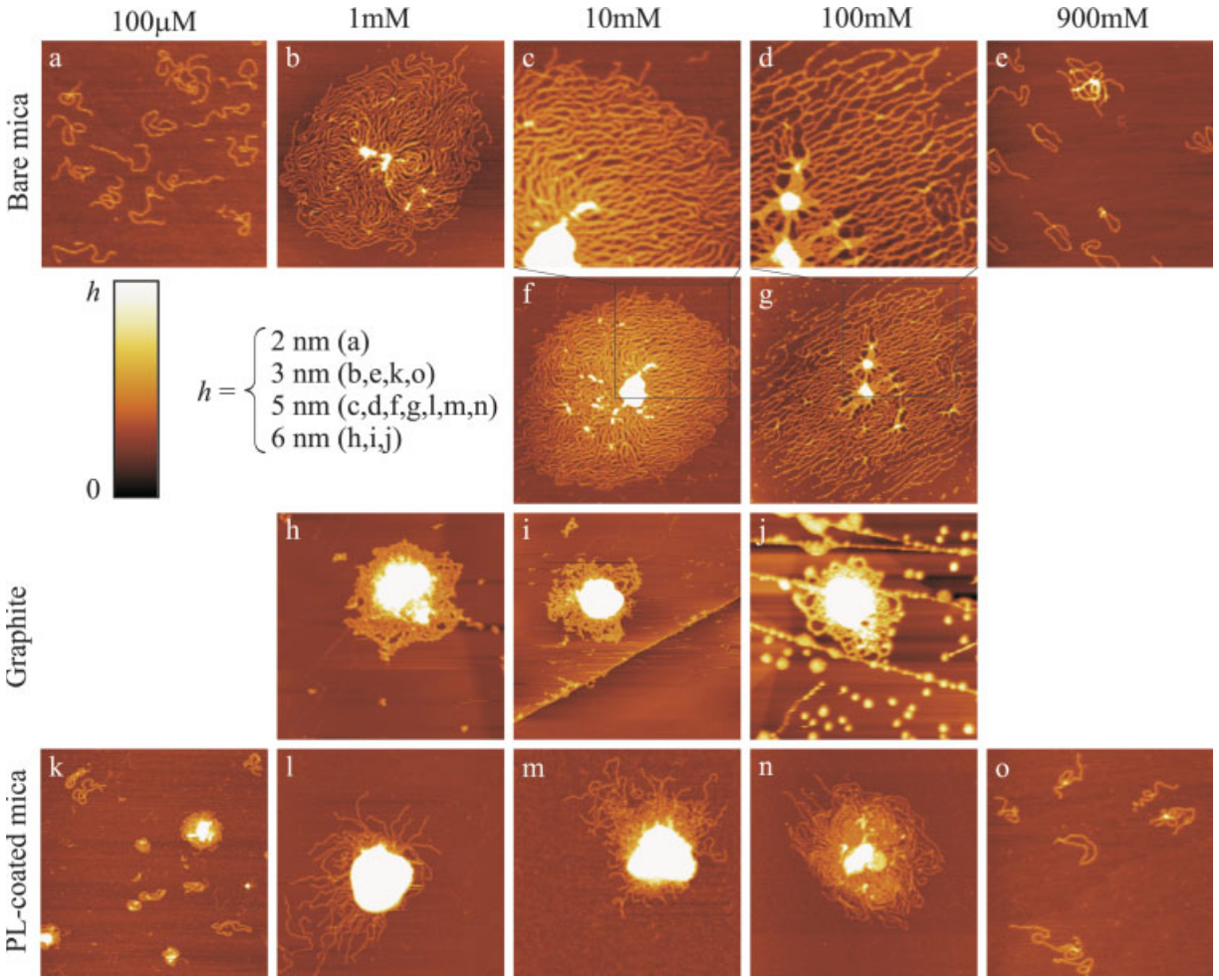

FIGURE 1 AFM images in air of DNA condensates prepared with different concentrations of spermidine as indicated above the images on bare mica (a–g), graphite (h–j) and PL-coated mica (k–o). Images (a–e) and (h–o) are 1×1 μm^2. Images (f) and (g) are 2×2 μm^2. Images (c) and (d) show additional details of the condensates in images (f) and (g), respectively.

2% uranyl acetate (Sigma) solution after which the sample was dipped in ethanol and blotted dry.

RESULTS AND DISCUSSION

Figures 1a–1g shows AFM images in air of DNA condensed with different concentrations of spermidine and deposited on bare mica. The morphology of the DNA changes dramatically with increasing multivalent-ion concentration. In zero or a very low concentration of spermidine (1 μM, data not shown), DNA does not adsorb to negatively charged mica. In contrast, at 10 μM (not shown) and 100 μM (Figure 1a) spermidine, individual uncondensed molecules are seen to adsorb to the surface. The multivalent ions thus mediate a net attraction between negatively charged mica and DNA. At 1, 10, and 100 mM (Figures 1b–1d, respectively), large multimolecular condensates are observed. The structures are disordered and do not resemble toroids or rods, but rather the previously reported flower-like structures. They are also very flat, consisting for the most part of bundles of several DNA molecules lying in direct contact with the surface. A higher three-dimensional core is also observed. At 900 mM spermidine (Figure 1e), the highest concentration investigated, the condensates are dissolved and uncondensed DNA is again observed. This well-known reentrant behavior was first reported by Pelta et al.[31]

Figures 1h–1j shows characteristic images of DNA condensates prepared in the same manner with spermidine but adsorbed on graphite instead of mica. Uncondensed DNA binds only weakly to the hydrophobic graphite and can

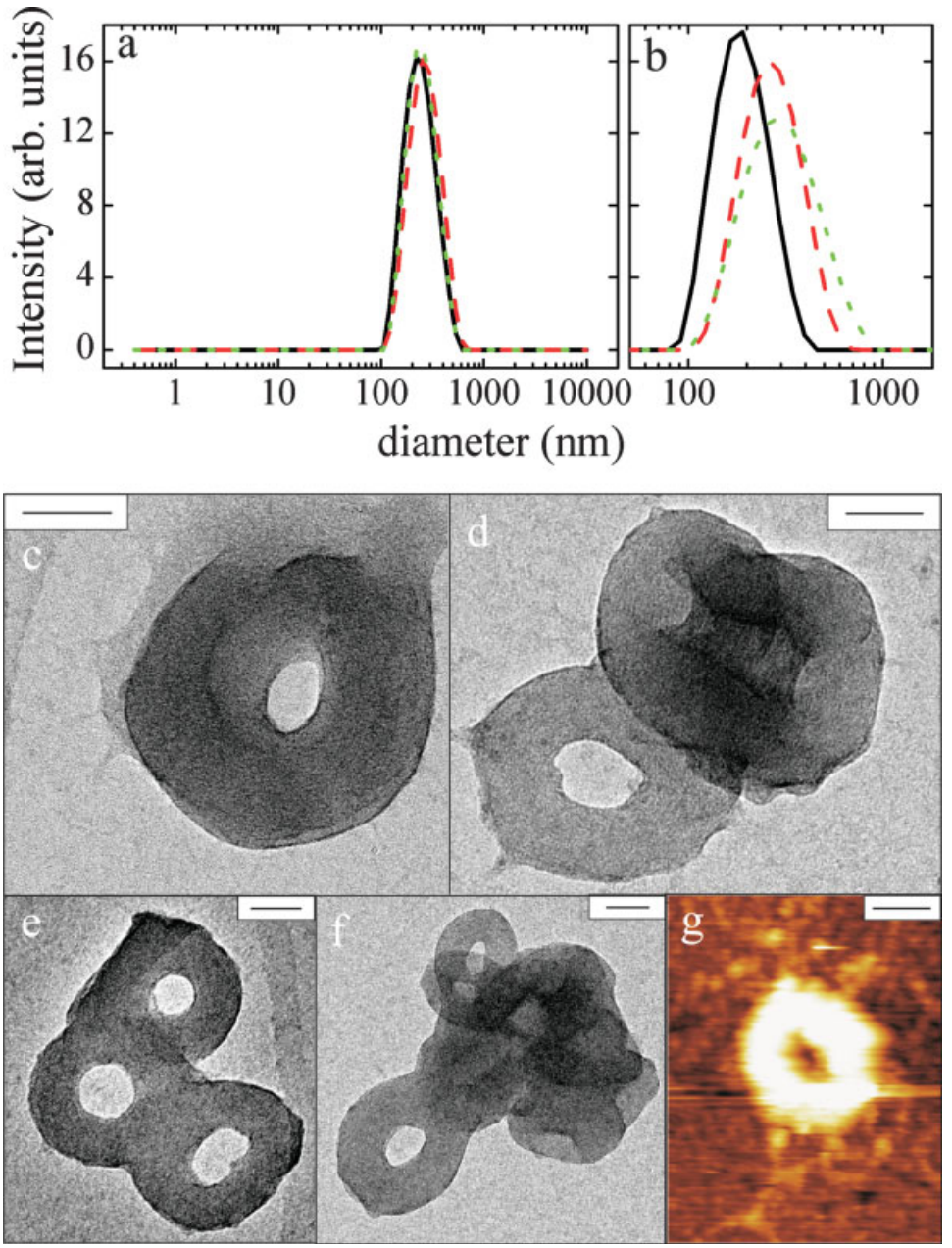

FIGURE 2 (a) Distribution of the hydrodynamic diameter of condensates in a solution containing 1 ng/μL DNA, 10 m*M* TRIS, and spermidine concentrations of 1 m*M* (solid line), 10 m*M* (dashed line), and 100 m*M* (dotted line) after 5 min incubation time measured with DLS. (b) Similar measurements for a solution containing 1 ng/μL DNA, 10 m*M* spermidine, and 10 m*M* TRIS after 2 min (solid line), 5 min (dashed line) and 8 min (dotted line) incubation time. Intensity is normalized to the area under the curve. (c–f) TEM images of DNA condensed with 1 m*M* spemidine in 10 m*M* TRIS. (g) AFM image of a toroidal DNA condensate on graphite treated with oxygen plasma. The color scale is the same as in Fig. 1, with $h = 6$ nm. All scalebars represent 50 nm.

therefore not be imaged well. Condensed DNA does get sufficiently immobilized on the graphite to obtain reliable images. Condensates are observed on the surface from above 0.1 m*M* spermidine to about 100 m*M*, a range of concentrations similar to that for bare mica. On the other hand, the morphology of the condensates is very different from that observed on bare mica: the core of the condensates appears globular, with greater height (up to $\sim$ 20 nm) and a smaller

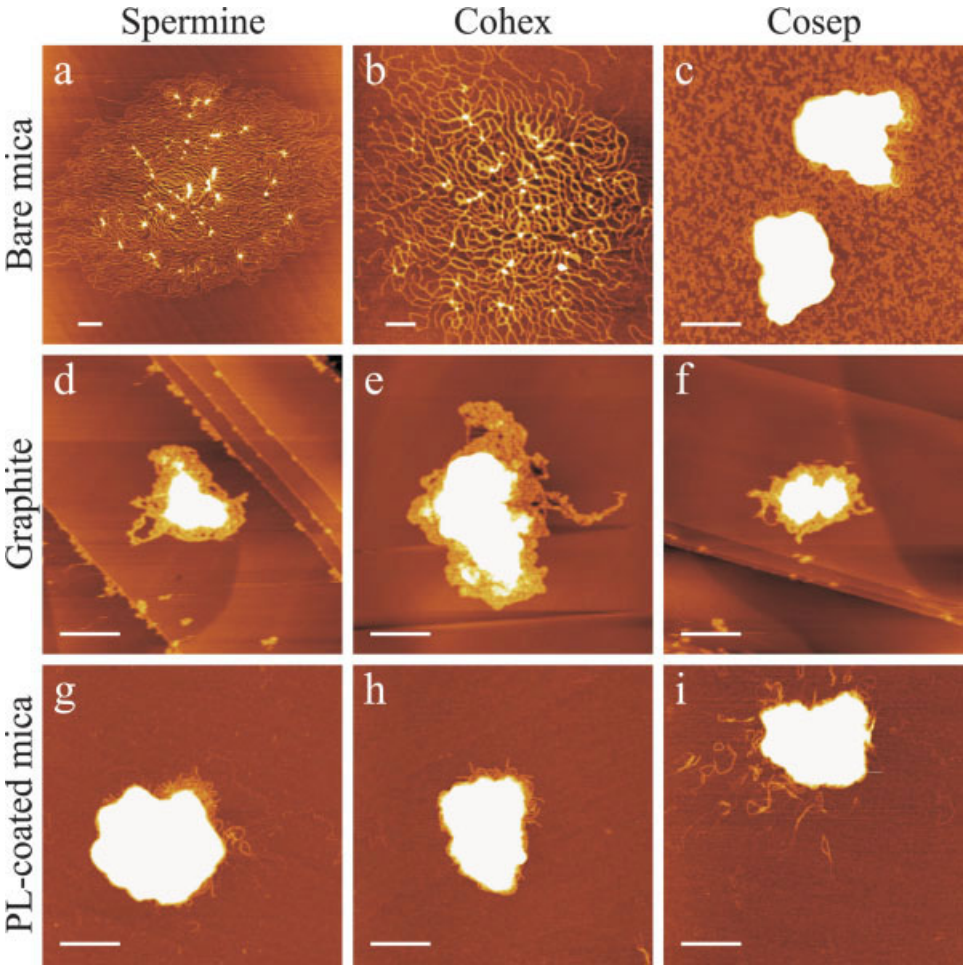

FIGURE 3 AFM images in air of DNA condensates prepared with 10 m*M* spermine (a, d, g), cohex (b, e, h), and cosep (c, f, i) on bare mica (a–c), on graphite (d–f), and on PL-coated mica (g–i). The cosep, and to a lesser extend the cohex, left behind a residue on bare mica at concentrations above 0.1 m*M*; this is the origin of the surface roughness in (c). All scalebars represent 200 nm. The color scale is the same as in Figure 1, with $h = 3$ nm for images (a) and (b) and 5 nm for images (c–i).

width than on mica. A flat disk structure is still observed surrounding the central globular core, but it does not extend as far from the core.

For comparison, Figures 1k–1o shows corresponding images for PL-coated mica. As expected for this positively charged surface, uncondensed DNA molecules already adsorb at low concentrations of spermidine (not shown). Small condensates are already visible on the surface at 10 μM (similar-looking to the smallest condensates in Figure 1k) and 100 μM (Figure 1k) spermidine, whereas condensates are not yet visible on bare mica at 100 μM. Finally, the condensates on PL-coated mica are three-dimensional with flat edges reminiscent of condensates observed on graphite, as seen in Figures 1l–1n. Since PL is a known condensing agent,[25] PL desorption from the surface might assist in the condensation and could cause the lower threshold for condensation on PL-coated mica. Because of this potential influence of PL, the results on this surface cannot be directly compared to the two other surfaces. Nonetheless, the similarities between graphite and PL-coated mica indicate that the net influence of these surfaces on condensate morphology is similar. The condensates on all three surfaces have comparable volumes as measured by AFM, confirming that they correspond to the same bulk structures before adsorption to the surface.

To ascertain to what extent the imaging surfaces disturb the three-dimensional structure of the condensates in solution, we performed DLS measurements on the same solu-

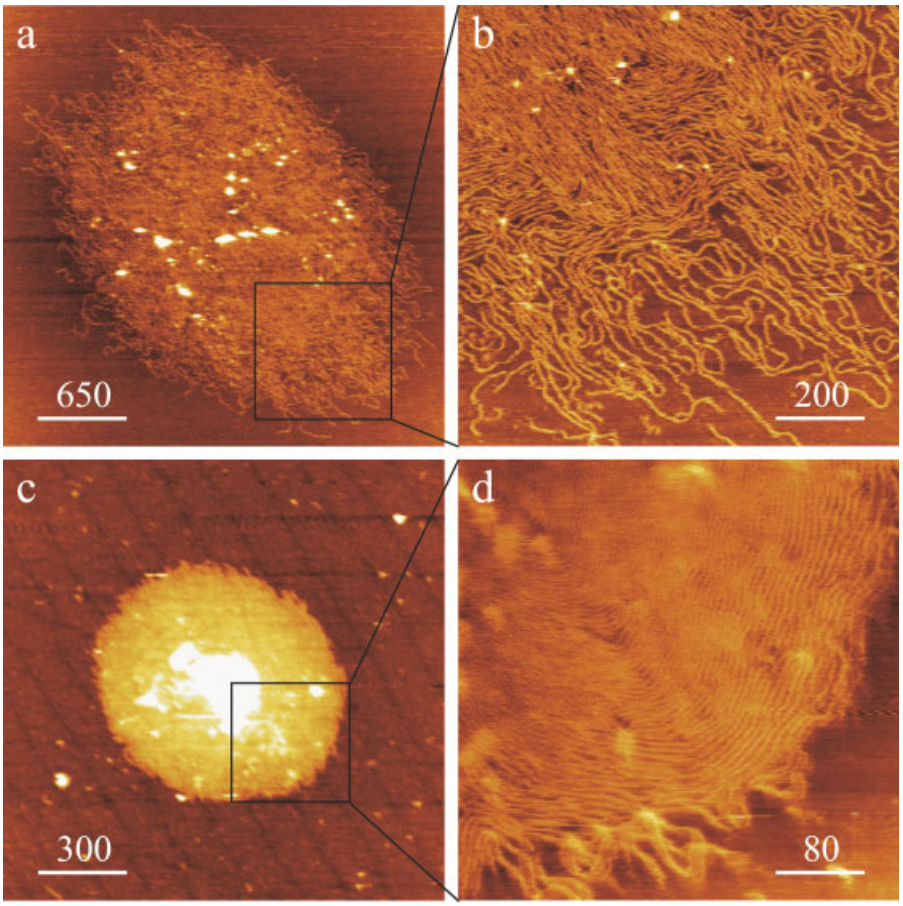

FIGURE 4 AFM images in liquid of DNA condensates on bare mica (a, b) and on PL-coated mica (c, d). All images were obtained in a solution containing 1 m*M* spermidine and 10 m*M* TRIS buffer. The color scale is the same as in Figure 1, with $h = 3$ nm. Images (b) and (d) show zooms of the condensates in images (a) and (c) respectively. Size of scalebars is given in nm.

tions as used for AFM imaging. Figure 2a shows the measured hydrodynamic-diameter distribution of DNA condensates prepared with 1, 10, and 100 m*M* spermidine after a 5 min incubation time. A well-defined, reproducible peak in the distribution is observed at 300 nm. The hydrodynamic diameter became larger with incubation time, indicating slow growth, or aggregation of the condensates (Figure 2b). The measured hydrodynamic diameters are in agreement with those obtained from comparable studies in the literature,[17] and the hydrodynamic diameter measured after 5 min incubation time is similar to the width of the DNA condensates observed on graphite and on PL-coated mica. For spermidine concentrations up to 0.1 m*M* and from 300 m*M* we did not obtain a well defined and reproducible size distribution, suggesting that DNA condensation did not occur.

To further investigate the morphology of the condensates in solution, we performed TEM imaging of DNA condensed with 1 m*M* spermidine. TEM mainly showed small aggregates of toroidal structures (Figures 2d–2f), consistent in size with the DLS measurement. Three-dimensional, well-condensed particles were thus present in solution. Individual toroids were also observed (Figure 2c).

As a further check of the existence of toroids in the solutions used for AFM imaging, we obtained AFM data on a graphite surface treated with oxygen plasma. The treatment was performed at 100 mTorr ($\sim$ 80% oxygen) for 15 s. This created a rough surface similar to that of a standard TEM grid. Toroidal structures could occasionally be observed on this carefully tuned surface with 0.25 m*M* spermidine as condensing agent, as shown in Figure 2g.

The spectrum of observations on the various surfaces together with the independent characterization of the samples by DLS and TEM directly demonstrate that the morphology of DNA condensates is significantly distorted by adsorption to a surface. Attractive DNA-surface interactions exist for all surfaces investigated, independently of the sign of the surface charge.

Counter-intuitively, the negatively charged bare mica surface perturbs the three-dimensional structure of the condensates the most and results in the flattest morphologies, indicating a strong attraction with negatively charged DNA. This attraction, like DNA condensation itself, is mediated by multivalent cations since no adhesion of DNA is observed in their absence. It is therefore likely that the same microscopic mechanism is responsible for both effects. It has been proposed that DNA condensation is driven by spatial correlations between multivalent ions.[9,10] This mechanism is however not restricted to DNA–DNA interactions and is expected to mediate attractive interactions between like-charged objects in general; Pastre et al.[32] recently presented a simple model for the specific case of DNA-surface interactions. The theory predicts that increasing the surface charge density enhances the correlations-induced attraction. Since bare mica has a bare surface charge density greater than that of DNA, it can potentially cause a surface-DNA attraction stronger than the attraction between DNA molecules.[32] Our observations that bare mica disturbs the bulk condensate structure the most and results in the most flattened structures are consistent with this interpretation.

We repeated these experiments using three other multivalent ions. Figure 3 shows results for 10 m*M* multivalent ions. The results for spermine and cohex were similar to those for spermidine, including the difference in the morphology of the condensates on bare mica, on graphite and on PL-coated mica (Figures 3a, 3b, 3d, 3e, 3g, and 3h). In contrast, the condensates prepared with cosep were similar for these three surfaces and resembled the structures observed on graphite and on PL-coated mica for the other ions (Figures 3c, 3f, and 3i). This indicates that the influence of the surface on the observed morphology is to some degree ion specific.

The measurements discussed earlier were performed in air, leaving open the possibility that the observed surface dependence is an artifact resulting from the drying process. To investigate the influence of drying we also performed AFM imaging in liquid. Figure 4 shows representative results for DNA condensed with 1 m*M* spermidine using bare mica and PL-coated mica as the imaging surfaces. Again a clear difference between condensates on bare mica (Figures 4a and 4b) and on PL-coated mica (Figures 4c and 4d) is observed, with similar trends in liquid as in air. On bare mica, the condensates are flat and often consist of only a DNA monolayer, indicating that the surface has a large influence on the morphology. On the PL-coated mica the condensates consist of a three-dimensional core surrounded by a flat disk.

Additional fine details of the condensates can be observed in liquid, in particular the arrangement of individual DNA molecules in the monolayer-thick region near the edges of the condensates. Further differences between condensate structures on the two surfaces exist at this more microscopic level. On PL-coated mica, DNA strands tend to be highly ordered, with adjacent molecules running parallel to each other. The spacing between strands is larger than that corresponding to tight packing ($\sim$ 2.4 nm[13]). For example, the spacing between parallel molecules in Figure 4d is 4 nm near the center of the condensate and 7 nm near the edges. On bare mica the DNA is less ordered and the spacing between individual molecules is larger than on PL-coated mica. Crossings of two DNA molecules are relatively rare, suggesting substantial relaxation of the condensate structure following adsorption.

CONCLUSIONS

We have imaged DNA condensed with different concentrations of four multivalent ions adsorbed on three chemically distinct surfaces. The flattened morphology of the condensates is indicative of strong DNA-surface interactions. We further observed significant systematic differences in the morphology of condensates adsorbed on different surfaces. Surprisingly, the negatively charged bare-mica surface results in the most flattened condensates. Graphite still perturbs the condensate structure somewhat; however, as can be seen from the flat edges adhering to the surface around the central globular condensates. Although it is possible to image weakly distorted condensates, very careful surface tuning is necessary to derive information on the morphology of undistorted condensates.

This study directly demonstrates that AFM imaging on surfaces is an unreliable probe of the morphology of condensates in bulk solution, limiting the usefulness of AFM for the study of DNA condensation with multivalent ions. DNA compaction near a charged surface is biologically relevant and interesting in its own right.[14] Our measurements however show that in such study it is crucial to use the precise surface of interest since the choice of surface influences the condensate structure.

The authors thank H. W. Zandbergen for providing access to the TEM and C. Dekker for general support.

REFERENCES

1. Bloomfield, V. Biopolymers 1997, 44, 269–282.
2. Gosule, L.; Schellman, J. Nature 1976, 259, 333–335.
3. Thomas, T.; Thomas, T. Cell Mol Life Sci 2001, 58, 244–258.
4. Vijayanathan, V.; Thomas, T.; Thomas, T. Biochemistry 2002, 41, 14085–14094.
5. Gelbart, W.; Bruinsma, R.; Pincus, P.; Parsegian, V. Phys Today 2000, 53, 38–44.
6. Golestanian, R.; Liverpool, T. Phys Rev E 2002, 66, 051802.

7. Kornyshev, A.; Leikin, S. Phys Rev Lett 1999, 82, 4138–4141.
8. Oosawa, F. Biopolymers 1968, 6, 1633.
9. Rouzina, I.; Bloomfield, V. J Phys Chem 1996, 100, 9977–9989.
10. Shklovskii, B. Phys Rev Lett 1999, 82, 3268–3271.
11. Chattoraj, D.; Gosule, L.; Schellman, J. J Mol Biol 1978, 121, 327–337.
12. Widom, J.; Baldwin, R. J Mol Biol 1980, 144, 431–453.
13. Hud, N.; Downing, K. Proc Natl Acad Sci USA 2001, 98, 14925–14930.
14. Hansma, H. Annu Rev Phys Chem 2001, 52, 71–92.
15. Fang, Y.; Hoh, J. J Am Chem Soc 1998, 120, 8903–8909.
16. Lin, Z.; Wang, C.; Feng, X.; Liu, M.; Li, J.; Bai, C. Nucleic Acids Res 1998, 26, 3228–3234.
17. Vijayanathan, V.; Thomas, T.; Antony, T.; Shirahata, A.; Thomas, T. Nucleic Acids Res 2004, 32, 127–134.
18. Liu, D.; Wang, C.; Lin, Z.; Li, J.; Xu, B.; Wei, Z.; Wang, Z.; Bai, C. Surf Interface Anal 2001, 32, 15–19.
19. Andrushchenko, V.; Leonenko, Z.; Cramb, D.; van de Sande, H.; Wieser, H. Biopolymers 2001, 61, 243–260.
20. Sitko, J.; Mateescu, E.; Hansma, H. Biophys J 2003, 84, 419–431.
21. Allen, M.; Bradbury, E.; Balhorn, R. Nucleic Acids Res 1997, 25, 2221–2226.
22. Chim, Y.; Lam, J.; Ma, Y.; Armes, S.; Lewis, A.; Roberts, C.; Stolnik, S.; Tendler, S.; Davies, M. Langmuir 2005, 21, 3591–3598.
23. Danielsen, S.; Varum, K.; Stokke, B. Biomacromolecules 2004, 5, 928–936.
24. Dunlap, D.; Maggi, A.; Soria, M.; Monaco, L. Nucleic Acids Res 1997, 25, 3095–3101.
25. Hansma, H.; Golan, R.; Hsieh, W.; Lollo, C.; Mullen-Ley, P.; Kwoh, D. Nucleic Acids Res 1998, 26, 2481–2487.
26. Fang, Y.; Yang, J. J Phys Chem B 1997, 101, 441–449.
27. Feng, Y.; Hoh, J. Nucleic Acids Res 1998, 26, 588–593.
28. Ono, M.; Spain, E. J Am Chem Soc 1999, 121, 7330–7334.
29. Besteman, K.; Zevenbergen, M.; Heering, H.; Lemay, S. Phys Rev Lett 2004, 93, 170802.
30. Besteman, K.; Zevenbergen, M.; Lemay, S. Phys Rev E 2005, 72, 061501.
31. Pelta, J.; Livolant, F.; Sikorav, J. J Biol Chem 1996, 271, 5656–5662.
32. Pastre, D.; Hamon, L.; Landousy, F.; Sorel, I.; David, M.; Zozime, A.; Le Cam, E.; Pietrement, O. Langmuir 2006, 22, 6651–6660.

Reviewing Editor: Kenneth Breslauer